The Relation between Eddy-Induced Transport and Isopycnic Gradients of Potential Vorticity

DAVID P. MARSHALL

Department of Meteorology, University of Reading, Reading, United Kingdom

RICHARD G. WILLIAMS

Oceanography Laboratories, University of Liverpool, Liverpool, United Kingdom

MEI-MAN LEE

James Rennell Division, Southampton Oceanography Centre, Southampton, United Kingdom

(Manuscript received 29 September 1997, in final form 18 August 1998)

ABSTRACT

The dynamical control of the eddy-induced transport is investigated in a series of idealized eddy-resolving experiments. When there is an active eddy field, the eddy-induced transport is found to correlate with isopycnic gradients of potential vorticity, rather than gradients of layer thickness. For any unforced layers, the eddy transfer leads to a homogenization of potential vorticity and a vanishing of the eddy-induced transport in the final steady state.

1. Introduction

Geostrophic eddies provide an advective transport of tracers in the atmosphere (Plumb and Mahlman 1987) and in the ocean (Gent et al. 1995). Recently, there has been much activity in developing parameterizations of the eddy-induced transport for coarse-resolution ocean models. An important issue that remains unresolved is whether the eddy-induced transport is related to gradients of isopycnic layer thickness, as advocated by Gent et al. (1995), or isopycnic gradients of potential vorticity, as advocated by Treguier et al. (1997). In this note, we conduct a series of controlled eddy-resolving numerical experiments, which confirm that the eddy-induced transport is determined by the isopycnic gradients of potential vorticity; this result is consistent with two previous case studies by Lee et al. (1997) and Treguier (1999).

2. Eddy-induced transport

Consider the transport of a water mass $h\mathbf{u}$ within an isopycnal layer of thickness h and velocity $\mathbf{u}$. Decomposing the variables into time mean and transient components, $h = \overline{h} + h'$, $\mathbf{u} = \overline{\mathbf{u}} + \mathbf{u}'$, where the overbar represents a time filter over several eddy life cycles, the time-mean transport is

$$\overline{h\mathbf{u}} = \overline{h}\,\overline{\mathbf{u}} + \overline{h'\mathbf{u}'} = \overline{h}(\overline{\mathbf{u}} + \mathbf{u}^*). \tag{1}$$

Here $(\overline{\mathbf{u}} + \mathbf{u}^*)$ is termed the ''transport velocity'' (Gent et al. 1995) and $\mathbf{u}^* \equiv \overline{h'\mathbf{u}'}/\overline{h}$ is the ''bolus velocity'' (Rhines 1982).

Within the oceanographic literature, the eddy contribution to the time-mean transport in (1) is usually identified with the bolus contribution $\overline{h}\mathbf{u}^*$. However, eddies influence the time-mean transport by changing both the thickness fluxes and the background velocity through Reynolds stresses (Greatbatch 1998). Thus, the ''eddy-induced transport'' is properly defined as the sum of the Reynolds and bolus transports

$$(\overline{h\mathbf{u}})_{\text{eddy}} = \overline{h}(\mathbf{u}_{\text{Reynolds}} + \mathbf{u}^*), \tag{2}$$

where

$$(\overline{h\mathbf{u}})_{\text{noneddy}} = \overline{h}(\overline{\mathbf{u}} - \mathbf{u}_{\text{Reynolds}}) \tag{3}$$

is the ''noneddy transport'' and

$$\overline{h}\mathbf{u}_{\text{Reynolds}} = \frac{\overline{h}}{(f + \overline{\zeta})}\left\{-\overline{\zeta'\mathbf{u}'} + \mathbf{k} \times \boldsymbol{\nabla}\frac{\overline{\mathbf{u}' \cdot \mathbf{u}'}}{2}\right\} \tag{4}$$

is the the transport generated by the eddy Reynolds

Corresponding author address: Dr. David P. Marshall, Department of Meteorology, University of Reading, P.O. Box 243, Reading RG6 6BB, United Kingdom.
E-mail: davidm@met.reading.ac.uk

stresses (see appendix). In the limit $|h'/\overline{h}| \ll 1$, the linearized Ertel potential vorticity flux[1] is

$$\overline{Q'\mathbf{u}'} \simeq \frac{\overline{\zeta'\mathbf{u}'}}{\overline{h}} - \overline{h'\mathbf{u}'}\frac{(f+\overline{\zeta})}{\overline{h}^2}$$

$$= -\frac{(f+\overline{\zeta})}{\overline{h}}(\mathbf{u}_{\text{Reynolds}} + \mathbf{u}^*) + \frac{1}{\overline{h}}\mathbf{k}\times\boldsymbol{\nabla}\frac{\overline{\mathbf{u}'\cdot\mathbf{u}'}}{2}, \quad (5)$$

where $Q = (\zeta + f)/h$ is the Ertel potential vorticity, f is the planetary vorticity, and ζ is the relative vorticity. Thus, the eddy-induced transport in (2) may be rewritten as

$$(\overline{h\mathbf{u}})_{\text{eddy}} \simeq -\frac{\overline{h}^2}{(f+\overline{\zeta})}\overline{Q'\mathbf{u}'} + \frac{\overline{h}}{(f+\overline{\zeta})}\mathbf{k}\times\boldsymbol{\nabla}\frac{\overline{\mathbf{u}'\cdot\mathbf{u}'}}{2}. \quad (6)$$

This transport includes a contribution proportional to the eddy flux of potential vorticity and a contribution directed around contours of eddy kinetic energy. Note that the eddy-induced transport in (6) is proportional to the eddy forcing of the momentum equation in the three-dimensional transformed Eulerian-mean formulation of Lee and Leach (1996) and Greatbatch (1998).

The contribution of the eddy kinetic energy term to the eddy-induced transport in (6) is generally small, except in atmospheric storm tracks (Hoskins 1983) and possibly in oceanic boundary currents and jets (Cronin 1996; Bowerman and Leach 1997). On the large scale in the ocean, we therefore assume that the eddy-induced transport is dominated by the eddy potential vorticity flux along isopycnals,

$$(\overline{h\mathbf{u}})_{\text{eddy}} \simeq -\frac{\overline{h}^2}{(f+\overline{\zeta})}\overline{Q'\mathbf{u}'}. \quad (7)$$

If we assume that potential enstrophy cascades to small scales where it is dissipated, then the eddy potential vorticity flux must on average be directed down the mean potential vorticity gradient (Rhines and Holland 1979), suggesting the closure[2]

$$\overline{Q'\mathbf{u}'} = -\kappa\boldsymbol{\nabla}\overline{Q}, \quad (8)$$

where κ is an eddy transfer coefficient and $\overline{Q} \cong (f + \overline{\zeta})/\overline{h}$. Then (7) can be rewritten as

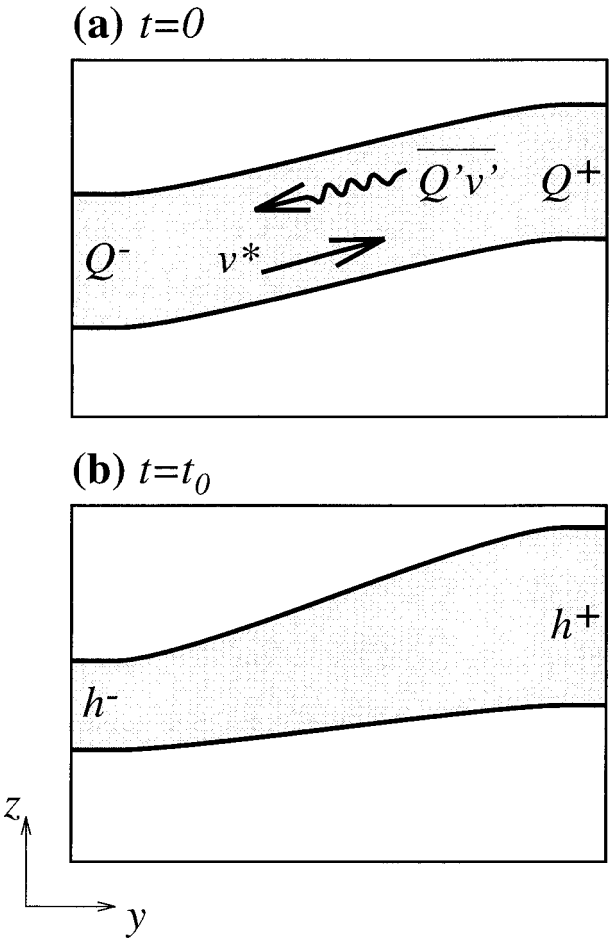

FIG. 1. A thought experiment illustrating the physical relation between the eddy flux of potential vorticity and the eddy-induced transport. (a) At time $t = 0$, the shaded isopycnic layer contains a uniform layer thickness and hence low values of potential vorticity Q^- at low latitudes, and high values of potential vorticity Q^+ at high latitudes. (b) At time $t = t_0$, the downgradient potential vorticity transfer $\overline{Q'v'}$ has led to a decreased layer thickness h^- at low latitudes, and an increased layer thickness h^+ at high latitudes. Thus, there has been an eddy-induced transfer of fluid from low to high latitudes v^* concomitant with the downgradient transfer of potential vorticity.

$$(\overline{h\mathbf{u}})_{\text{eddy}} \simeq \kappa\frac{\overline{h}}{\overline{Q}}\boldsymbol{\nabla}\overline{Q}. \quad (9)$$

A similar relation to (9) connecting the bolus transport and potential vorticity gradient has been suggested by Treguier et al. (1997).

A physical interpretation of (9) is given in the following thought experiment. Consider an isopycnal layer initially having uniform layer thickness and a poleward potential vorticity gradient (Fig. 1a). Assuming that the isopycnal layer adjusts due to eddies fluxing potential vorticity downgradient, then the layer thickness is reduced at low latitudes and increased at high latitudes (Fig. 1b). This change in layer thickness implies a poleward eddy-induced transport, concomitant with the downgradient transfer of potential vorticity.

[1] More generally, one can write an unapproximated form of (5) using the identity,

$$\frac{\overline{hQ''\mathbf{u}''}}{\overline{h}} \equiv \frac{\overline{\zeta'\mathbf{u}'}}{\overline{h}} - \frac{\overline{h'\mathbf{u}'}(f+\overline{\zeta})}{\overline{h}^2}$$

(Greatbatch 1998), where $Q'' = Q - \overline{hQ}/\overline{h}$, $\mathbf{u}'' = \mathbf{u} - \overline{h\mathbf{u}}/\overline{h}$, represent departures from thickness-weighted means. While the formulation in terms of thickness-weighted means is appealing from a physical standpoint and requires no approximation, we have opted to use standard Eulerian averages in the main text in the interests of simplifying the mathematical presentation.

[2] In general, (8) applies to the *divergent* component of the eddy potential vorticity flux (Marshall and Shutts 1981). The larger rotational component of the eddy potential vorticity flux can be directed both up and down the mean potential vorticity gradient; see Holland and Rhines (1980) and Marshall (1984).

3. Numerical experiments

We now examine the relation between the eddy-induced transport and isopycnal gradients of potential vorticity by conducting a series of eddy-resolving experiments in a zonally periodic channel. We focus on a special case where the time-mean meridional transport is dominated by the eddy-induced contribution and the noneddy contribution is close to zero.

a. Model configuration

The model is described in Lee et al. (1997), and consists of three isopycnal layers, configured in a zonally periodic channel of meridional extent 1600 km and zonal extent 600 km, with 10-km resolution. There is no mechanical forcing, but layer interfaces are restored to prescribed values within 200-km-wide ''relaxation zones'' adjacent to the northern and southern boundaries in order to maintain a zonal jet. The model is integrated for 18 years, and diagnostics are obtained from the final 6 years of integration.

A series of four experiments is presented in which the potential vorticity gradient in the middle layer is $\partial\overline{Q}_2/\partial y \approx -\beta/H$, 0, β/H and $2\beta/H$; here $\beta \equiv df/dy = 2 \times 10^{-11}$ m^{-1} s^{-1} is the planetary vorticity gradient and $H = 500$ m is the mean thickness of the middle layer.

b. Meridional transport

The meridional streamfunction for the time-mean transport velocity ($\overline{v} + v^*$) is shown in Fig. 2. In this zonal integration, the streamfunction for the time-mean transport in (1) is dominated by the eddy-induced transport in (2)—see Table 1. The gross structure of the streamfunction appears to be similar in each case: there is poleward transport in the surface layer and equatorward transport in the bottom layer. In these layers, the eddy-induced transport is directed down the background thickness gradient, and up the background potential vorticity gradient, consistent with both thickness and potential vorticity closures for the eddy-induced transport.

The eddy-induced transport in the middle layer, however, varies strongly between the four experiments. The transport is consistently directed up the potential vorticity gradient. In the case of potential vorticity decreasing poleward, the transport in the middle layer is equatorward (Fig. 2a); in the case of uniform potential vorticity, the transport in the middle layer is vanishingly small (Fig. 2b); and in the case of uniform thickness, the transport in the middle layer is poleward (Fig. 2c). In each case, contribution of the eddy kinetic energy term in (6) to the eddy-induced transport is negligible, and the eddy-induced transport is therefore equivalent to the weighted eddy potential vorticity flux.

Scatterplots of the meridional transport within the unforced interior of the middle layer are shown in Fig. 3

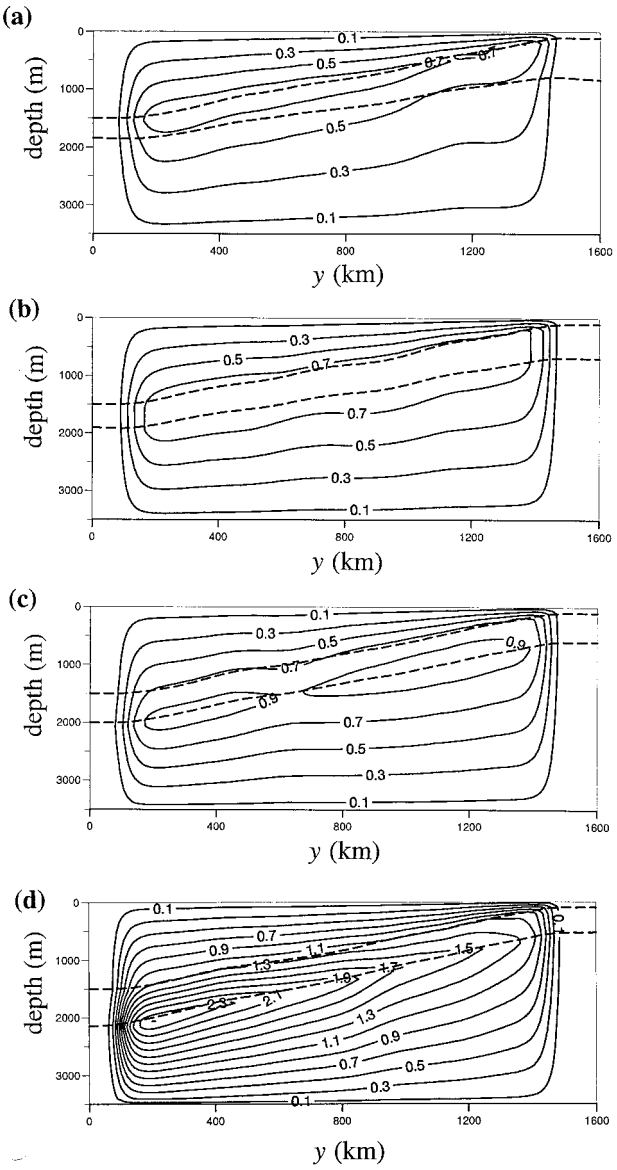

FIG. 2. Meridional streamfunction (full lines) for the total transport $\psi = \int (\overline{v} + v^*)\, dz$ (m^2 s^{-1}) evaluated from a time average along isopycnals over years 13–18 for four different integrations with different potential vorticity gradients in the middle layer: (a) $\partial\overline{Q}/\partial y = -\beta/H$; (b) uniform potential vorticity $\partial\overline{Q}/\partial y = 0$; (c) uniform thickness $\partial\overline{Q}/\partial y = \beta/H$; and (d) $\partial\overline{Q}/\partial y = 2\beta/H$. The dashed lines are the layer interfaces, which are strongly relaxed to their initial height in zones of width 200 km adjacent to the northern and southern boundaries. Note how the total transport in the middle layer is equatorward in (a), nearly zero in (b), and poleward in (c) and (d).

against the mean gradients in potential vorticity and thickness. Figure 3a reveals a clear monotonic relation between the eddy-induced transport and mean potential vorticity gradient, consistent with (9); this relation is particularly evident in experiment d, where the large variation in $(\overline{hv})_{\text{eddy}}$ across the channel is a consequence of the integration not having reached a statistically steady state. In contrast, Fig. 3b indicates that the re-

TABLE 1. Mean and standard deviation for meridional transport ($m^2\ s^{-1}$) by the bolus velocity $\overline{h}v^*$, the Reynolds velocity $\overline{h}v_{\text{Reynolds}}$, and noneddy velocity $\overline{h}(\overline{v} - v_{\text{Reynolds}})$ (evaluated between $y = 400$ and 1200 km) for integrations with (i) uniform potential vorticity and (ii) uniform thickness in the middle layer. The standard deviations give an indication of the strength of the confined meridional cells, embedded within the larger-scale overturning cell. In this zonal integration, the Reynolds velocity is dominated entirely by the eddy flux of absolute vorticity, as assumed in section 2c; the contribution of the eddy kinetic energy term in (4) is vanishingly small.

	$\overline{h}v^*$	$\overline{h}v_{\text{Reynolds}}$	$\overline{h}(\overline{v} - v_{\text{Reynolds}})$
(i) $\partial\overline{Q}_2/\partial y = 0$			
Layer 1	0.828 ± 0.154	−0.015 ± 0.170	−0.001 ± 0.021
Layer 2	0.013 ± 0.013	−0.005 ± 0.015	0.000 ± 0.003
Layer 3	−0.833 ± 0.153	−0.009 ± 0.034	0.024 ± 0.177
(ii) $\partial\overline{Q}_2/\partial y = \beta/H$			
Layer 1	0.798 ± 0.153	−0.034 ± 0.137	0.003 ± 0.018
Layer 2	0.236 ± 0.016	−0.007 ± 0.013	−0.005 ± 0.003
Layer 3	−1.025 ± 0.155	−0.015 ± 0.023	0.049 ± 0.143

lation between the eddy-induced transport and mean thickness gradient is offset due to the gradients in planetary vorticity and mean relative vorticity

$$(\overline{hv})_{\text{eddy}} \simeq \frac{\kappa}{\overline{Q}}\left(\beta + \frac{\partial\overline{\zeta}}{\partial y}\right) - \kappa\frac{\partial\overline{h}}{\partial y}, \qquad (10)$$

obtained by expanding (9). Moreover, the variation of $\partial\overline{\zeta}/\partial y$ across the channel leads to increased scatter between the transport and thickness gradient (Fig. 3b), compared with a reduced scatter between the transport and potential vorticity gradient (Fig. 3a).

Meridional streamfunctions for the bolus and Eulerian-mean velocities are shown in Figs. 4a and 4b for the case of uniform potential vorticity in the middle layer. At leading order, the large-scale transport is dominated by the bolus contribution (Fig. 4a and Table 1), as argued by Treguier et al. (1997). However, on the scale of the inertial Rhines jets embedded within the larger-scale current (Rhines 1975), the Eulerian-mean transport consists of a series of confined meridional cells, in places providing up to 40% of the total transport (Fig. 4b and Table 1). These Eulerian-mean cells are dominated by the Reynolds velocity in the upper two layers and a frictional velocity in the bottom layer. In the middle layer with uniform potential vorticity, the Reynolds and bolus velocities oppose each other and both become small (Fig. 4c) such that the total eddy-induced transport vanishes. However, this cancellation between the Reynolds and bolus velocities occurs only in the case of uniform potential vorticity, and the bolus velocity is an order of magnitude larger with a nonzero background potential vorticity gradient (see Table 1).

4. Implications for the large-scale distribution of potential vorticity

In the previous experiments, a background potential vorticity gradient has been imposed and maintained through relaxation of the interface heights at the northern and southern boundaries. We consider a more realistic case with unforced deeper layers to determine the impact of the eddy-induced transport on the large-scale potential vorticity field. A four-layer, eddy-resolving model is used where only the height of the interface separating the upper two layers is maintained within the relaxation zones (in order to supply available potential energy and sustain the eddy field). The initial interface heights are shown in Fig. 5a (dashed lines): the upper layer thins poleward, the two middle layers each have a uniform thickness of 500 m, and the bottom layer thickens poleward accordingly. Otherwise the model details are identical to the previous three-layer experiments.

Initially, the meridional streamfunction for the transport velocity reveals an overturning cell with intense poleward flow in the upper layer and equatorward return flow in the bottom layer (Fig. 5a). Within the middle layers of initial uniform thickness, the eddy-induced transport is weaker and broadly poleward, directed up the initial potential vorticity gradient. However, a more complex pattern is seen adjacent to the relaxation zones in the upper middle layer: here, partial slumping of the lower interface over the 2-yr averaging period leads to reversed potential vorticity gradients and a reversal in the eddy-induced transport. The large-scale meridional overturning forces the unforced layer interfaces to slump, deepening to the north and shallowing to the south, as shown by the interface heights averaged between years 25 and 30 (Fig. 5b, dashed lines).

The resulting potential vorticity distributions for the initial state and a snapshot at the end of year 30 are shown for each layer in Fig. 6. Initially, the potential vorticity gradient is poleward in the upper three layers and equatorward in the bottom layer. After 30 yr, the potential vorticity gradient in the upper two layers is confined to diffusive boundary layers adjacent to relaxation zones. Note that the potential vorticity gradient reverses in the upper middle layer, due to the forcing of its upper interface within the relaxation zones. The potential vorticity becomes nearly uniform in the lower two layers. The degree of homogenization, measured here by the ratio of the final potential vorticity gradient

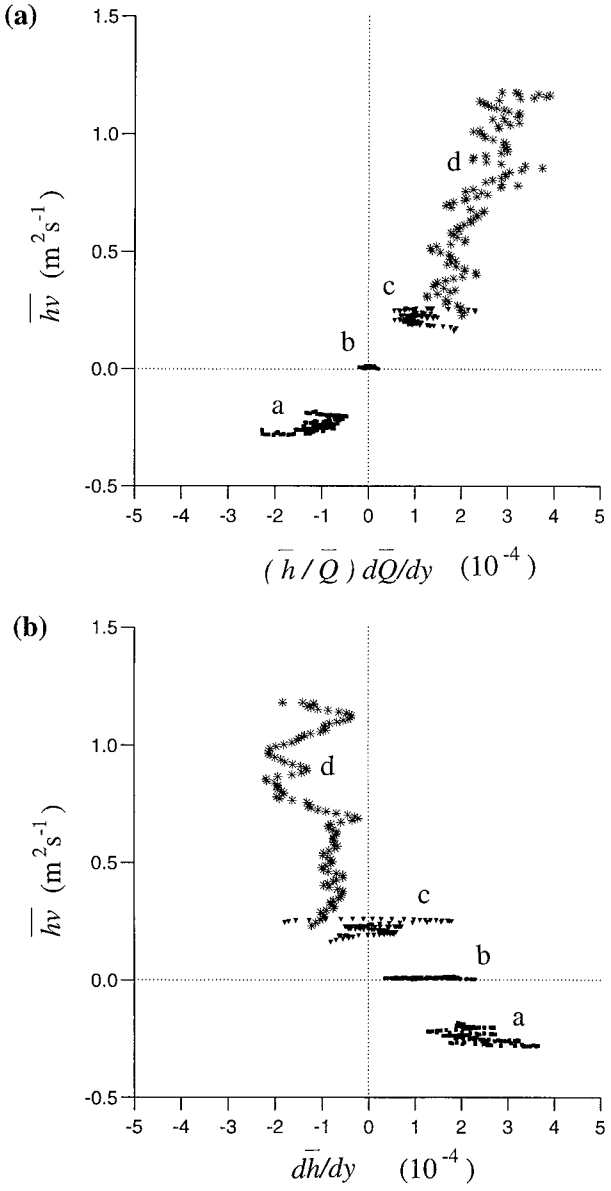

FIG. 3. Scatterplots showing the total transport $\overline{hv}$ in the middle layer (m^2 s^{-1}) against (a) the weighted potential vorticity gradient $(\overline{h}/\overline{Q})\partial\overline{Q}/\partial y$ (10^{-4}) and (b) the thickness gradient $\partial\overline{h}/\partial y$ (10^{-4}). The values are shown for each integration in Fig. 2, with squares for case a, circles for case b, triangles for case c, and stars for case d. Each point represents a zonal average of the quantities with values taken in the unforced interior from $y = 200$ to 1400 km.

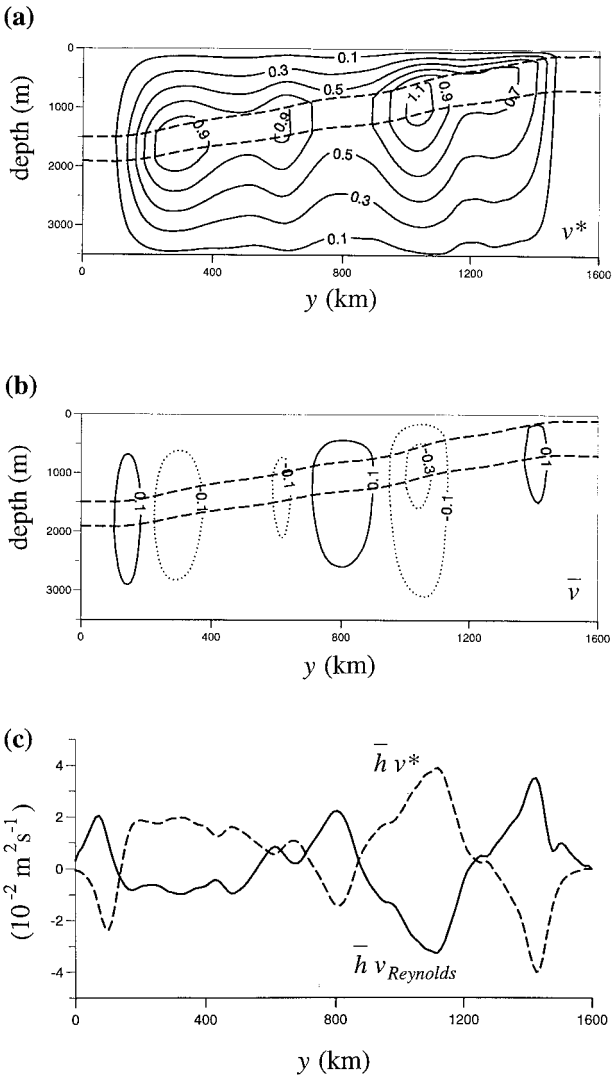

FIG. 4. Meridional streamfunctions (m^2 s^{-1}) for (a) the bolus velocity and (b) the Eulerian-mean velocity in the case of uniform potential vorticity in the middle layer; (c) graphs of the bolus (dashed line) and Reynolds (solid line) velocities (10^{-2} m^2 s^{-1}) within the middle layer. The localized cells in the Eulerian-mean streamfunction are opposed by variations in the bolus streamfunction, which leads to the single large-scale meridional cell for the total transport shown in Fig. 2b. The Eulerian-mean streamfunction is dominated by the Reynolds velocity in the upper two layers and by a frictional velocity in the lower layer (Table 1). Note that the cancellation of the bolus and Reynolds transport in the middle layer is a special case for uniform potential vorticity and that the bolus transport becomes an order of magnitude larger when the potential vorticity is nonuniform (see Table 1).

to the potential vorticity gradient associated with the β variation for a uniform layer thickness $(dQ/dy)_{\text{final}}/(\beta/H)$, is 0.02 and 0.01 in the lower middle and bottom layers, respectively. Associated with this change in the potential vorticity structure is a dramatic weakening in meridional transport, as shown in Fig. 5b (full lines). The meridional transport becomes confined to the upper two layers and vanishes in the bottom two layers with nearly uniform potential vorticity.

Thus, this experiment demonstrates how the eddy-induced transport acts to homogenize the large-scale potential vorticity field, consistent with the conceptual picture presented in Fig. 1 and previous quasigeostrophic studies (Rhines and Young 1982; Marshall et al. 1993). This end state of nearly uniform potential vorticity will only generally be achieved in a non-eddy-

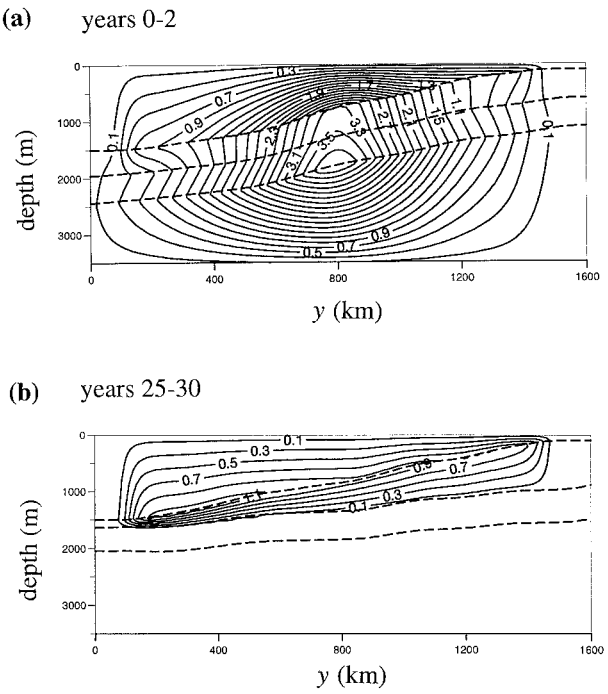

FIG. 5. Meridional streamfunction (full lines) for the total transport ($m^2\ s^{-1}$) and interface height (dashed lines) from the four-layer eddy-resolving experiment. Only the upper interface is restored to its initial height in the relaxation zones: (a) time average between years 0 and 2; (b) time average between years 25 and 30. Note how the deeper layers slump, leading to the overturning cell weakening and becoming confined to the upper two layers.

resolving model if the eddy-induced transport is parameterized in terms of the gradient in potential vorticity, rather than layer thickness.

5. Conclusions

Eddies provide a rectified transport of water masses through both the Reynolds and bolus velocities. To date, attempts to parameterize this eddy-induced transport have focused purely on the contribution of the bolus velocity. In particular, there has been much debate over whether the bolus velocity should be parameterized in terms of gradients of isopycnal thickness or isopycnic gradients of potential vorticity.

Our numerical experiments indicate that the eddy-induced transport should be parameterized in terms of isopycnic gradients of potential vorticity. On the large scale, the eddy-induced transport is dominated by the bolus transport; locally, however, the Reynolds transport is not negligible, consisting of a series of confined meridional cells that contribute up to 40% of the total eddy-induced transport.

A difficulty in employing a potential vorticity closure is that it should only be employed in regions of significant eddy activity. For example, a stagnant abyssal ocean containing flat isopycnals and no eddies should not adjust to a state of uniform potential vorticity. However, Killworth (1997) has addressed this issue by developing a potential vorticity closure in which the eddy transfer coefficient is derived from linear instability theory and vanishes in the limit of flat isopycnals. A more serious limitation of a potential vorticity closure may be over variable bottom topography, where eddies can flux potential vorticity upgradient—see, for example, the discussion of Holloway (1997); more work is required to address this issue.

While the eddy-induced transports predicted using either isopycnic thickness or potential vorticity closures are similar whenever there are significant thickness gradients, the end state arising from using these different closures is very different. Only employing a potential vorticity closure leads to an end state of uniform potential vorticity (as argued by Rhines and Young 1982). Using our eddy-resolving isopycnic model, we obtain an end state of uniform potential vorticity for any unforced layers (see Fig. 6). In the case of uniform potential vorticity, the eddy-induced transport vanishes with the bolus transport opposing the Reynolds transport. This result is particularly pertinent given the observations of nearly uniform potential vorticity occurring over much of the main thermocline (McDowell et al. 1982) and even parts of the abyssal ocean (O'Dwyer and Williams 1997).

Acknowledgments. Comments on a preliminary draft from Peter Gent, Richard Greatbatch, Greg Holloway, George Nurser, Rick Smith, and two anonymous reviewers are gratefully acknowledged. This study was supported by the Natural Environment Research Council GR3/10157 (DPM) and NERC UK WOCE Special Topic GST/02/1686 (RGW).

APPENDIX

Derivation of the Reynolds Transport

The momentum equation within an isopycnal layer can be written

$$\frac{\partial \mathbf{u}}{\partial t} + (f + \zeta)\mathbf{k} \times \mathbf{u} + \nabla\left(\frac{M}{\rho} + \frac{\mathbf{u}\cdot\mathbf{u}}{2}\right) = \mathcal{F}, \quad \text{(A1)}$$

where ∇ is the gradient operator evaluated along an isopycnal, M is the Montgomery potential, ρ is density, and $\mathcal{F}$ is mechanical forcing. Taking the time mean of (A1) and rearranging for the Eulerian-mean transport gives

$$\overline{h}\overline{\mathbf{u}} = \frac{\overline{h}}{(f + \overline{\zeta})}\mathbf{k} \times \left\{\frac{\partial \overline{\mathbf{u}}}{\partial t} + \nabla\left(\frac{\overline{M}}{\rho_0} + \frac{\overline{\mathbf{u}}\cdot\overline{\mathbf{u}}}{2}\right) - \mathcal{F}\right\} + \frac{\overline{h}}{(f + \overline{\zeta})}\left\{-\overline{\zeta'\mathbf{u}'} + \mathbf{k} \times \nabla\frac{\overline{\mathbf{u}'\cdot\mathbf{u}'}}{2}\right\}. \quad \text{(A2)}$$

Thus, the component of the Eulerian-mean transport driven directly by the eddy "Reynolds stresses" is

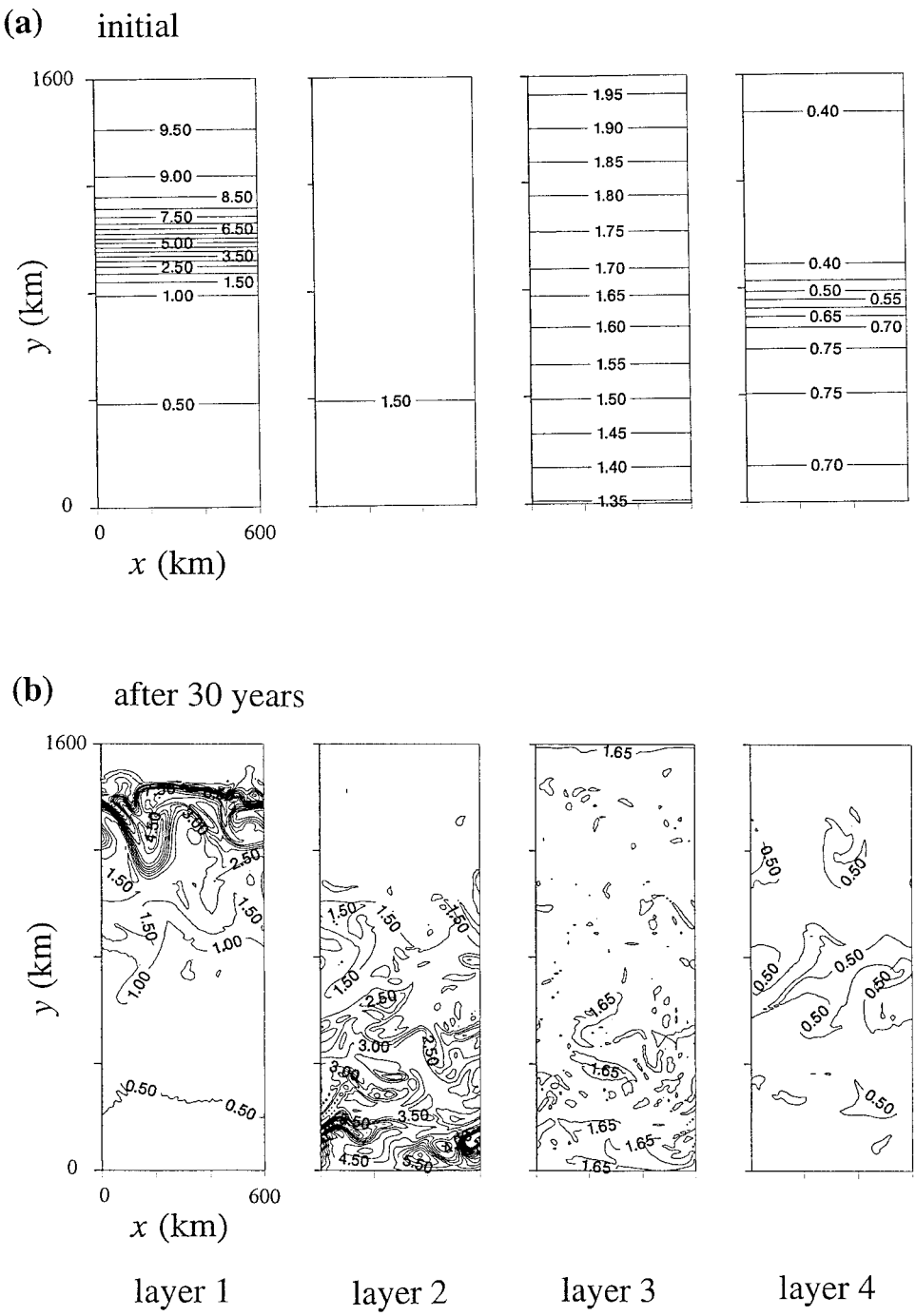

FIG. 6. Potential vorticity distribution (10^{-7} m^{-1} s^{-1}) for the four-layer eddy-resolving experiment at (a) year 0 and (b) the end of year 30. The maintenance of the upper interface and slumping of the remaining interfaces leads to the potential vorticity gradient becoming enhanced in the upper middle layer. In the lower two layers, the eddy-induced transport acts to remove the potential vorticitiy gradient: after 30 yr the potential vorticity in these layers is nearly uniform (note the greatly enhanced contour interval). Note that the eddy-induced transport consequently vanishes in the lower two layers toward the end of the integration (Fig. 5b).

$$\overline{h}\mathbf{u}_{\text{Reynolds}} = \frac{\overline{h}}{(f + \overline{\zeta})}\left\{-\overline{\zeta'\mathbf{u}'} + \mathbf{k} \times \nabla\frac{\overline{\mathbf{u}' \cdot \mathbf{u}'}}{2}\right\}, \quad \text{(A3)}$$

consistent with (4).

REFERENCES

Bowerman, S. J., and H. Leach, 1997: Eddies in the northeastern North Atlantic: Statistics from observations from a moving ship. *J. Geophys. Res.,* **102,** 23 041–23 062.

Cronin, M., 1996: Eddy-mean flow interaction in the Gulf Stream at 68°W. Part II: Eddy forcing on the time-mean flow. *J. Phys. Oceanogr.,* **26,** 2132–2151.

Gent, P. R., J. Willebrand, T. J. McDougall, and J. C. McWilliams, 1995: Parameterizing eddy-induced tracer transports in ocean circulation models. *J. Phys. Oceanogr.,* **25,** 463–474.

Greatbatch, R. J., 1998: Exploring the relationship between eddy-induced transport velocity, vertical momentum transfer, and the isopycnal flux of potential vorticity. *J. Phys. Oceanogr.,* **28,** 422–432.

Holland, W. R., and P. B. Rhines, 1980: An example of eddy induced ocean circulation. *J. Phys. Oceanogr.,* **10,** 1010–1031.

Holloway, G., 1997: Eddy transport of thickness and momentum in layer and level models. *J. Phys. Oceanogr.,* **27,** 1153–1157.

Hoskins, B. J., 1983: Modelling of the transient eddies and their feedback on the mean flow. *Large-Scale Dynamical Processes in the Atmosphere,* B. J. Hoskins and R. Pearce, Eds., Academic Press, 169–199.

Killworth, P. D, 1997: On the parameterisation of eddy transfer. Part I: Theory. *J. Mar. Res.,* **55,** 1171–1197.

Lee, M.-M., and H. Leach, 1996: Eliassen–Palm flux and eddy potential vorticity flux for a nonquasigeostrophic time-mean flow. *J. Phys. Oceanogr.,* **26,** 1304–1319.

——, D. P. Marshall, and R. G. Williams, 1997: On the eddy transfer of tracers: Advective or diffusive? *J. Mar. Res.,* **55,** 483–505.

Marshall, J. C., 1984: Eddy-mean flow interaction in a barotropic ocean model. *Quart. J. Roy. Meteor. Soc.,* **110,** 573–590.

——, and G. J. Shutts, 1981: A note on rotational and divergent eddy fluxes. *J. Phys. Oceanogr.,* **11,** 1677–1680.

——, D. Olbers, H. Ross, and D. Wolf-Gladrow, 1993: Potential vorticity constraints on the dynamics and hydrography of the Southern Ocean. *J. Phys. Oceanogr.,* **23,** 465–487.

McDowell, S., P. B. Rhines, and T. Keffer, 1982: North Atlantic potential vorticity and its relation to the general circulation. *J. Phys. Oceanogr.,* **12,** 1417–1436.

O'Dwyer, J. E., and R. G. Williams, 1997: The climatological distribution of potential vorticity over the abyssal ocean. *J. Phys. Oceanogr.,* **27,** 2488–2505.

Plumb, R. A., and J. D. Mahlman, 1987: The zonally averaged transport characteristics of the GFDL General Circulation Model. *J. Atmos. Sci.,* **44,** 298–327.

Rhines, P. B., 1975: Waves and turbulence on a β-plane. *J. Fluid Mech.,* **69,** 417–443.

——, 1982: Basic dynamics of the large-scale geostrophic circulation. *Summer Study Program in Geophysical Fluid Dynamics,* Woods Hole, MA, Woods Hole Oceanographic Institution, 1–47.

——, and W. R. Holland, 1979: A theoretical discussion of eddy-driven mean flows. *Dyn. Atmos. Oceans,* **3,** 289–325.

——, and W. R. Young, 1982: Homogenisation of potential vorticity in planetary gyres. *J. Fluid Mech.,* **122,** 347–368.

Treguier, A. M., 1999: Evaluating eddy mixing coefficients from eddy resolving models: A case study. *J. Mar. Res.,* **57,** 89–103.

——, I. M. Held, and V. D. Larichev, 1997: On the parameterization of quasi-geostrophic eddies in primitive equation ocean models. *J. Phys. Oceanogr.,* **27,** 567–580.